PARAMETRIC ANALYSIS OF ANISOTROPY IN STABLY STRATIFIED ROTATING HOMOGENEOUS TURBULENCE

F.S. Godeferd, L. Liechtenstein, C. Cambon
Lab. de Mécanique des Fluides et d'Acoustique UMR 5509, Ecole Centrale de Lyon, France
fabien.godeferd@ec-lyon.fr

ABSTRACT

We investigate the combined effects of rotation and stable stratification on homogeneous turbulence, which render the flow very anisotropic at all scales : coherent structures are deformed either to pancake- or cigar- like shapes. Accordingly, energy is distributed differently in spectral space depending on the relative amplitudes of rotation/stratification, but directional spectra exhibit anisotropy at almost all scales, down to the smallest. Moreover, using a poloidal/toroidal decomposition of the velocity, we show that an additional coupling mode appears in the strongly stratified case when even slow rotation is present, with respect to the purely stratified case.

INTRODUCTION

Homogeneous isotropic turbulence has been studied extensively with theoretical, experimental and numerical approaches. The knowledge of fundamental physical processes from these studies are built into models, which treat most complex flows, such as inhomogeneous or multiphase flows. The models assume local homogeneity and isotropy of turbulence at length scales smaller than a predefined cut-off scale. However, a lot of models which are based on isotropic turbulence are applied to flows with a systematic anisotropy. In these cases, even at very small scales isotropy of turbulence is a priori not guaranteed and according to our studies far from being fulfilled for stably stratified rotating turbulence.

The basic set of equations describing homogeneous rotating and stably stratified turbulence is the Boussinesq approximation in a rotating frame of reference. The fluctuating velocity field $\boldsymbol{u}$ and buoyancy field b are governed by

$$\partial_t \boldsymbol{u} - \nu\nabla^2\boldsymbol{u} = -\nabla p - \boldsymbol{u}\cdot\nabla\boldsymbol{u} - 2\Omega\,\boldsymbol{n}\times\boldsymbol{u} + b\,\boldsymbol{n} \qquad (1)$$

$$(\partial_t + \boldsymbol{u}\cdot\nabla)\,b - \chi\nabla^2 b = -N^2\boldsymbol{n}\cdot\boldsymbol{u}, \qquad (2)$$

where p, ν and χ are the compensated pressure, the kinematic viscosity and the thermal diffusivity respectively. We choose a Prandtl number of $\nu/\chi = 1$. And, due to incompressibility $\nabla\cdot\boldsymbol{u} = 0$. The two parameters characterizing stratification and rotation are N, the Brunt-Vaisala frequency, and Ω, the system rotation. A lot of works concentrate on either rotating [1, 2] or stratified [3, 4, 5, 6] turbulence. Here we will systematically explore rotating and stratified turbulence, therefore introducing the non-dimensional parameter $\alpha = 2\Omega/N$.

Linear solution of the Boussinesq equations

As both the buoyancy force and the Coriolis force act linearly on the flow field, fundamental properties of this system can already be studied with the linearized system of equations, which can be solved analytically due to the absence of the nonlinear advection term. They are often used as a basis for the developement of more complex models. The simplest representation of solutions are found in Fourier space, as pressure as well as mass conservation effects can be implicitly treated by using a projection operator. The solution of the system is done as an expansion of transverse plane waves

$$\hat{\boldsymbol{v}}(\boldsymbol{k},t) = \sum_{\epsilon=0,\pm1} \boldsymbol{\mathcal{N}}^{\epsilon} e^{-i\epsilon\sigma t}\left(\boldsymbol{\mathcal{N}}^{-\epsilon}\cdot\hat{\boldsymbol{v}}(\boldsymbol{k},0)\right) \qquad (3)$$

where $\boldsymbol{\mathcal{N}}^{\epsilon}$ are the eigenvectors of the linearized equations, and depend on $\boldsymbol{k}$. Accordingly, the dispersion relation $\sigma^2 = N^2\sin^2\theta + 4\Omega^2\cos^2\theta$ depends on the direction of the vector $\boldsymbol{k}$. Keeping in mind that equation 3 is the solution of the linearized Boussinesq equations, it can easily be seen that the velocity field is naturally decomposed in a *linearly* oscillating inertio-gravity wave part and a *linearly* time-independent vortex part. In meteorology, these two parts of the flow field are known as ageostrophic and quasigeostrophic parts respectively.

Divergence-free flows in Fourier space can be represented with two-components, as no velocity component along the wave vector $\boldsymbol{k}$ is possible. The Craya–Herring frame, a local frame of reference with unit vectors

$$\boldsymbol{e}^{(1)} = \frac{\boldsymbol{k}\times\boldsymbol{n}}{|\boldsymbol{k}\times\boldsymbol{n}|}\ ,\ \ \boldsymbol{e}^{(2)} = \frac{\boldsymbol{k}}{k}\times\boldsymbol{e}^{(1)}\ ,\ \ \boldsymbol{e}^{(3)} = \frac{\boldsymbol{k}}{k}. \qquad (4)$$

allows the decomposition of the three-component Cartesian velocity field into a new two-component field that correspond to a mathematical decomposition into a poloidal and a toroidal part. The buoyancy can be added to this vector as a fully imaginary third component, reducing the problem of solving the system in Fourier space for five unknown $\hat{u}_x$, $\hat{u}_y$, $\hat{u}_z$, $\hat{b}$, $\hat{p}$ to solving it for a three-component vector $\hat{\boldsymbol{v}}$. A further advantage of this system is that the new vector squared is proportional to the invariant of the system, the potential *and* kinetic energy combined, instead of a proportionality only to kinetic energy. Note, that the poloidal/toroidal decomposition differs for the general case from the wave/vortex decomposition outlined in the previous paragraph. They will only be identical for pure stratification.

These decompositions are also valid for the spectral 2^{nd}-order tensor Φ_{ij}, defined as

$$< \hat{u}_i^*(\boldsymbol{p},t)\hat{u}_j(\boldsymbol{k},t) > /2 = \Phi_{ij}(\boldsymbol{k},t)\delta(\boldsymbol{k}-\boldsymbol{p}). \qquad (5)$$

The linear evolution of energy from arbitrary initial conditions can therefore be analytically known using equation (3). However, the linear energy evolution is a complex problem which depends on the ratios of kinetic to potential energy and rotation to stratification. Even the asymptotic tendencies of energy transfers between the toroidal, poloidal and potential parts are not trivial. This shows the importance of a balanced energy budget in initialing the simulations, as anisotropy is otherwise created due to a simple asymmetry of energy on different modes. Nevertheless, if the velocity field is initially equipartitioned between the toroidal, poloidal and potential mode, no anisotropy can be created by linear mechanisms.

Direct numerical simulations

The formation of structures such as pancakes or cigars observed in dominantly stratified turbulence and dominantly rotating turbulence is only possible with nonlinear models. A variety of closure models have been tested on anisotropic turbulence, where statistical two-point closures such as the eddy-damped-quasi-normal-Markovian, the direct-interaction-approximation or the test-field model play a dominant role.

Although the statistical two-point models can reproduce a wide range of phenomena observed in rotating and stratified turbulence, they are based on assumptions, not necessary in direct numerical simulation (DNS). As we treat homogeneous turbulence, a fully de-aliased pseudo-spectral collocation method in a cubic box of length 2π with periodic boundary conditions is used.

Due to necessarily limited computer resources, the resolution and therefore the Reynolds number is limited. The high accuracy due to weak approximations but only moderate Reynolds numbers has to be compared to high-Reynolds number attainable with statistical models which include a degree of assumptions and hypotheses. Models are built to describe only certain statistical quantities, whereas DNS gives a series of full velocity fields, enabling the generation of statistical quantities directly from the flow field.

The flow field is initialized in Fourier space with a narrow-band energy spectrum and the time scheme is third-order Adams-Bashforth with exact integration of the viscous term. All DNS presented here are freely decaying. The buoyancy and system rotation are applied after an initial isotropic pre-calculation, so to a velocity field with fully established triple correlations. The abrupt introduction of an anisotropic force disequilibrates the flow field. The fluctuations in the statistics due to this discontinuity decay over a few turbulence turnover times. The runs use 512^3 collocation points and $Re_\lambda \approx 160$ for $\alpha = 10$ and $Re_\lambda \approx 120$ for $\alpha = 0.1$. Stably stratified and rotating turbulence exhibit the following features:

- The total dissipation of energy is reduced. The reduction is moderate for dominantly stratified turbulence and very high for dominantly rotating turbulence. This is an effect of less efficient cascading processes.

- Spontaneous formation of coherent structures from an initially isotropic turbulence field are shown in figure 1. Iso-enstrophy surfaces in dominantly stratified turbulence resemble horizontal pancakes while in dominantly rotating turbulence they resemble vertical cigars.

- The directional distribution of energy is altered. For dominantly stratified cases, the energy is concentrated in a thin vertical cone of Fourier space [6]. For dominantly rotating cases, the energy is concentrated quasi-horizontally, outside a flat cone of the Fourier space. However, even with very strong stratification or rotation, the energy distribution in Fourier space occupies a finite, non-vanishing volume, excluding a complete reduction to only horizontal velocity components or a complete two-dimensionalization of the velocity field.

- Directional spectra show a variety of scaling laws and a dependence of these laws on the direction apart from exhibiting a steeper spectrum and so a reduced cascade. The differences of spectra for different directions suggest that not only a shell-to-shell cascade has to be studied, but also a directional inside-one-shell cascade or a combination of the two can appear in anisotropic turbulence [4]. This is an effect of the different ways a vector triad can be constructed in anisotropic turbulence, compared to isotropic turbulence.

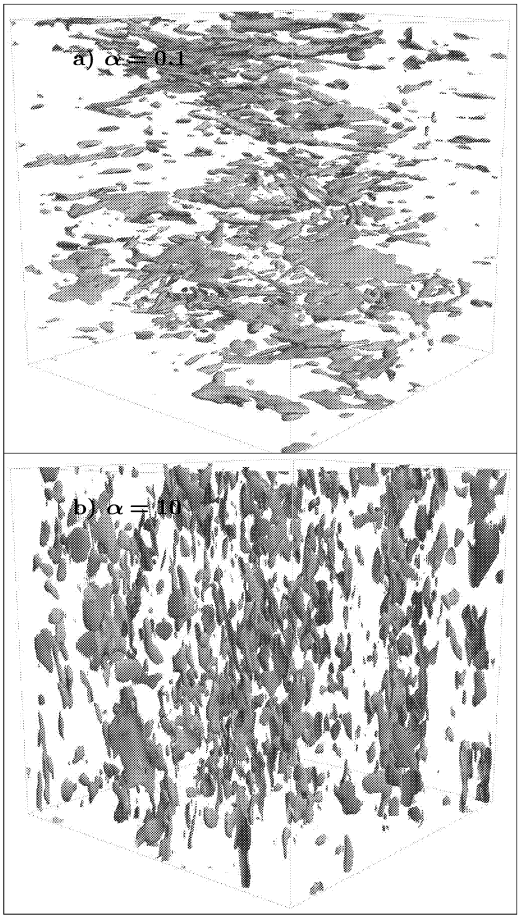

Figure 1: Iso-enstrophy surfaces of a dominantly stratified case (a) and a dominantly rotating case (b).

- The directional velocity correlation length scales, defined in the following section, show typical structures. Stratified turbulence exhibits normally growing horizontal scales but very short vertical scales. Scales in dominantly rotating turbulence show the opposite effect.

- The structure of the velocity fields has been found to arrange themselves in the following way.

  Dominantly stratified turbulence shows quasi-horizontal velocity fields which are decorrelated in the vertical. The velocity patterns due to waves are difficult to detect due to the dominance of the horizontal velocity components. The vertical component, however, is important for energy exchange mechanisms.

  Although the velocity field of dominantly rotating turbulence shows a columnar structuring, it does not favour a vertical or horizontal component of energy. Furthermore, although the horizontal velocity components in one column show little vertical variability, the vertical ones do show significant changes.

  Therefore, the velocity fields in stratified turbulence can be described as a quasi two-component 3D flow, while the description of rotating turbulence as three-component 2D velocity field might not be correct.

- The vorticity field of stratified turbulence shows dominance of the horizontal component, an effect of the shear layers between pancakes. Dominantly rotating turbulence shows a much higher vertical vorticity and a good

correlation in the vertical. So the vorticity vector field of rotating turbulence much more approaches a 2D field than the velocity vector field. Furthermore, the vorticity vector field shows an asymmetry between positive and negative vertical vorticity. This might be due to production of vorticity by system rotation.

- Anisotropy is found down to the smallest scales, and anisotropy due to rotation seems to be largest at these smallest scales. Therefore there is a need for anisotropic sub-scale models which can be used in in large eddy simulations where rotation or stratification is present.

EULERIAN STATISTICS

Directional Correlations Lengths

A good indicator of structural anisotropy in the flow are directional correlation length scales. Linear theory applied to initially isotropic data with equipartition of poloidal and potential energy strictly conserves isotropy of any single-time double correlations as it conserves the structure function. They are equal in horizontal and vertical directions, in contrast to results from full non-linear DNS. In isotropic turbulence, longitudinal length scales are twice cross correlation ones, so for easier comparison we show twice the magnitude of cross correlation length scales.

Velocity correlation lengths. These DNS results, shown in figure 2(a), can interpreted as directional integral length-scales and are defined as

$$L^n_{ii}(t) = \frac{1}{<u_i u_i>} \int_0^\infty < u_i(\boldsymbol{x}) u_i(\boldsymbol{x} + d\boldsymbol{x}_n) > d\boldsymbol{x}_n \qquad (6)$$

for horizontal velocity components u_i and different separation directions n (vertical and horizontal). As they are calculated by integrating a spectrum, they mainly show the anisotropy of the energy containing scale for the respective spectrum.

The elongation in the horizontal as well as the reduction in the vertical length scales clearly illustrate the pancake like structures observed for dominantly stratified runs in figure 1. Due to the high stratification of the DNS, the vertical scale decreases after an initial short increase and reaches a final value of close to 1/30 of the calculation box height. The horizontal length scale grows under the effect of energy decay to about 1/10 of the box length at the end of the run with no definite evolution law. The final ratio of the vertical to horizontal scale is approximately 3 for the case with $\alpha = 0.1$

Dominant rotation cases exhibit a scale elongation of L^z_{xx} in the vertical, illustrating the formation of vertically elongated structures shown in figure 1(b). The horizontal correlation lengths of the case with $\alpha = 10$. follow an evolution close to the isotropic case, although, in the latter, Reynolds numbers are 70% smaller than in the former. The ratio of vertical to horizontal length scales is approximately 3. The vertical velocity correlation length scale reaches values of up to one fifth of the box height. Validity of runs with large values of correlation lengths can be influenced by the periodic boundary conditions. However, due to no abrupt increase in scales, an effect expected due to vortex stretching, we believe that the run is still valid.

Vorticity correlation length scales. They are shown in figure 2(b) and defined similarly to equation 6, but by correlating vorticity instead of velocity. To find quantitative aspect ratios of enstrophy iso-surfaces as in figure 1, length scales based on vorticity rather than velocity are more appropriate. Similar to velocity correlation length scales representing energy

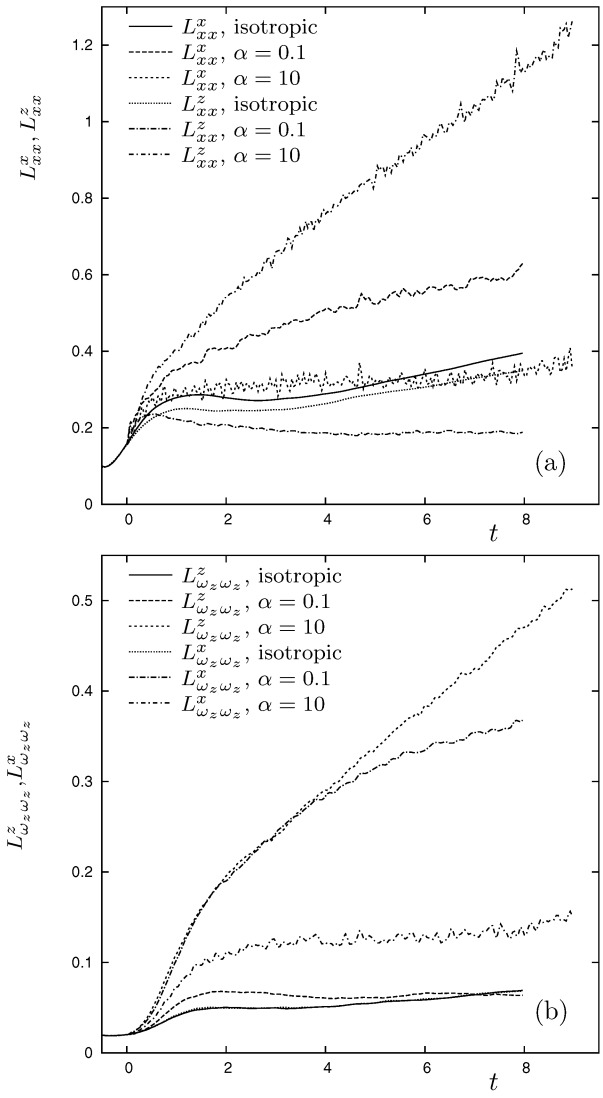

Figure 2: Time evolution of the directional velocity correlation length scales: dashed lines: L^x_{xx}, solid lines: L^z_{xx} Time evolution of the directional vorticity correlation length scales: dashed lines: $L^z_{\omega_z\omega_z}$, solid lines: $L^x_{\omega_z\omega_z}$.

containing scales, the vorticity correlation length scales are found close to the enstrophy containing scales, so characterizing anisotropy in the region of the Taylor micro scale.

Isotropic vorticity length scales tend to grow slower than the ones from anisotropic runs. Apart from illustrating pancakes and cigars shown in figures 1(a) and (b) respectively, the high anisotropy found in vorticity length scales illustrates the absence of isotropy even at scales close to the viscous range, underlining the fact that isotropic sub-grid models will encounter difficulties when modeling anisotropic turbulence. No asymptotic value seems to be reached for the sizes or aspect ratios of the structures. This implies that no asymptotic value is reached for small scale anisotropy.

The vertical length scale $L^z_{\omega_z\omega_z}$ is directly linked to vertical columns with average heights similar to the correlation length. The horizontal length scale $L^x_{\omega_z\omega_z}$ for rotation dominant cases can be interpreted as an average horizontal distance between two cigars, as the vertical vorticity is the dominant component of the total vorticity. This distance is growing significantly

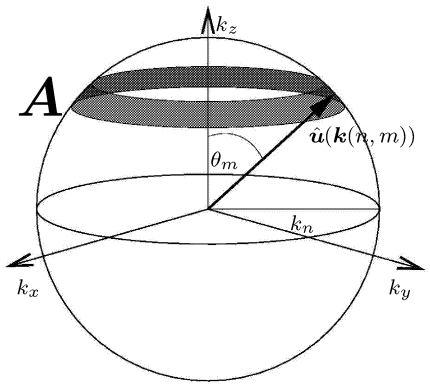

Figure 3: Integrating surface for angular dependent spectra.

faster than $L^x_{\omega_z\omega_z}$ in the isotropic case.

For dominantly stratified cases, the horizontal vorticity is dominating, so the correlation length of vertical vorticity might not be the dominant feature in the flow. However, $L^x_{\omega_z\omega_z}$ will still give an indication of the horizontal scale of structures. For dominant stratification, $L^z_{\omega_z\omega_z}$ grows at around the same rate as the isotropic case. Seemingly, this quantity has a connection with the thickness of the pancakes, but at a second look the thickness is more probably defined by vertical shear and so horizontal rather than vertical vorticity.

A surprising feature shown in figure 2(b) is the similar growth of the vertical correlation length $L^z_{\omega_z\omega_z}$ for dominant rotation and the horizontal correlation length $L^x_{\omega_z\omega_z}$ for dominant stratification. The means that pancake like structures, shown in figure 1, grow horizontally at roughly the same rate as cigar shaped like structures in the vertical.

Angular energy spectra

In contrast to isotropic turbulence, the transfer of energy over the polar angle θ in connection with transfers between the toroidal, poloidal and potential mode is of prime importance in the decay of anisotropic turbulence. Angular energy spectra defined as

$$E(k_n,\theta_m)=\frac{m}{2}\left[\int_{\theta_m-\Delta\theta/2}^{\theta_m+\Delta\theta/2}\cos\theta d\theta\right]^{-1}\sum_{|k|\epsilon I_n,\theta_k\epsilon J_m}\hat{\boldsymbol{u}}^*(\boldsymbol{k})\cdot\hat{\boldsymbol{u}}(\boldsymbol{k}) \quad (7)$$

are similar to spherically averaged spectra, but integrated only over a sector $\Delta\theta$ of a spherical shell shown in figure 3. Directional anisotropy of the energy distribution leads to spectra which do not collapse for different angles θ. On the other hand, polarization anisotropy leads to differences between toroidal, poloidal and potential spectra.

Dominant rotation. We show the toroidal, poloidal and potential directional spectra on figures 4a,b,c. For comparison, an isotropic spectrum is shown with dotted line. The curves marked $\cos\theta \approx 0$ correspond to quasi-horizontal directions and show cascade laws of around k^{-2}. The curves corresponding to quasi-vertical directions are marked $\cos\theta \approx 1$ and show cascade laws of around k^{-4}, which approaches slopes normally found in viscous ranges.

The main three observations to be made are the increased steepness of slopes compared to isotropic turbulence, the similarities between toroidal and poloidal parts and the highest anisotropy found at the largest wave numbers. This anisotropy attains more than five orders of magnitude difference between energy in the horizontal and vertical direction.

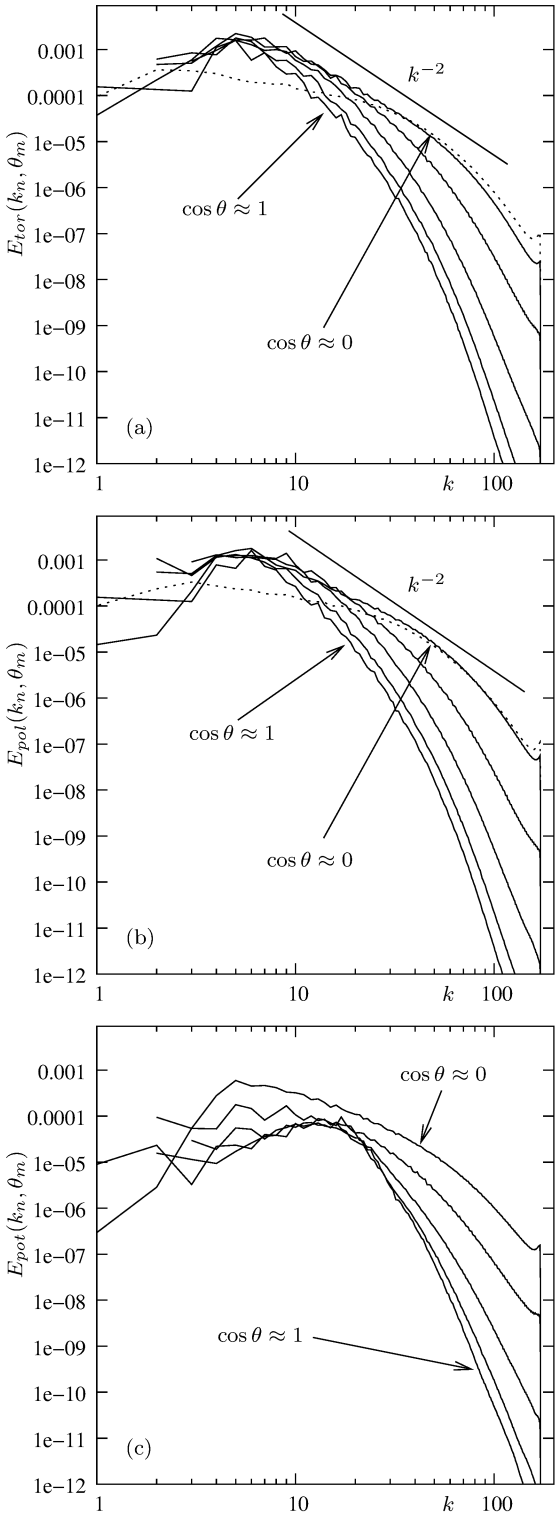

Figure 4: Poloidal (top), toroidal (middle) and potential (bottom) angular spectra for DNS run with $\alpha = 10$. Dotted curves show spherical spectra from the corresponding isotropic run for comparison.

The large anisotropy at small scales combined with the data presented in figure 2 indicates a trend toward a two-component vorticity field correlated in the vertical direction, with a vertically correlated three-component velocity field.

The total potential energy in figure 4(c) is about half an order magnitude smaller than the energy in either toroidal or poloidal mode. However, as the cascade of potential energy is more efficient than in either poloidal or toroidal mode, the potential energy density at smallest scales is of the same order of magnitude as the kinetic energy modes. In contrast to having simply a reduced cascade in cases with pure rotation, this mechanism succeeds in feeding kinetic energy back into the system at large k, after an intermediate transfer to the potential energy mode. In other words, the energy manages to bypass the normal cascade inside one mode in utilizing the more efficient cascade in the potential mode. This is possible, because of the efficient linear transfers of energy exchange between, on the on hand, potential and poloidal parts, and on the other hand poloidal and toroidal parts. To sum up, the parameter $\alpha = 10$ exhibits large scale mechanisms of energy cascade similar to the rotating case. However, the interaction of the poloidal mode with the potential mode allows a mechanism which generates turbulent kinetic energy at the smallest scales of the poloidal mode, without necessitating the normal cascading processes.

The Reynolds number is just large enough in the high resolution simulations to show trends concerning the slope of a possible inertial range. The spectra exhibit a range of different slopes between k^{-2} for the quasi-horizontal direction to k^{-4} for the quasi-vertical one. Standard spectra of rotating turbulence can therefore exhibit k^{-3} slopes without any mechanisms of 2D turbulence simply by averaging over all polar angles θ [7], which answers the two-dimentionalization question raised in some works (e.g. [1]). The spectra of the potential energy is smaller at larger scales due to the relatively weak stratification.

Dominant stratification. Figures 5a,b,c show the toroidal, poloidal and potential angular spectra for the run with $\alpha = 0.1$. Again, for comparison, we show an isotropic spectrum with dotted line. The curves marked $\cos\theta \approx 0$ correspond to spectra with a median angle of $\theta = 4\pi/10$ directions, the curves marked $\cos\theta \approx 1$ correspond to a median angle of $\theta = \pi/10$ and the other curves have ascending values for θ from top to bottom.

First, although the spectra are still steeper than their isotropic counterparts, they are less steep than in figure 4. Second, the poloidal and toroidal parts of the energy show large qualitative and quantitative differences, but the poloidal and potential parts of the energy show similarities, especially so in the horizontal direction. Third, with the exception of the vertical spectrum of potential energy, the anisotropy of the flow is found exclusively in the toroidal part of the velocity field at intermediate wave numbers. The rotation, which is an order of magnitude smaller than the stratification, takes effect after a considerably longer time. This is consistent with the fact that the system has had time to fulfill only four rotational periods compared to forty Brunt-Vaisala periods at the end of the run.

Similar to cases with pure stratification, the spectra of the vortex/toroidal mode exhibit slopes of approximately $k^{-3.5}$ for the quasi-horizontal spectrum in figure 5. The quasi-vertical parts have a maximum at larger k and a smoothly changing slope between largest and smallest scales. The maximum difference in spectral energy between the vertical and the horizontal direction is nearly four orders of magnitude, found in the toroidal spectrum.

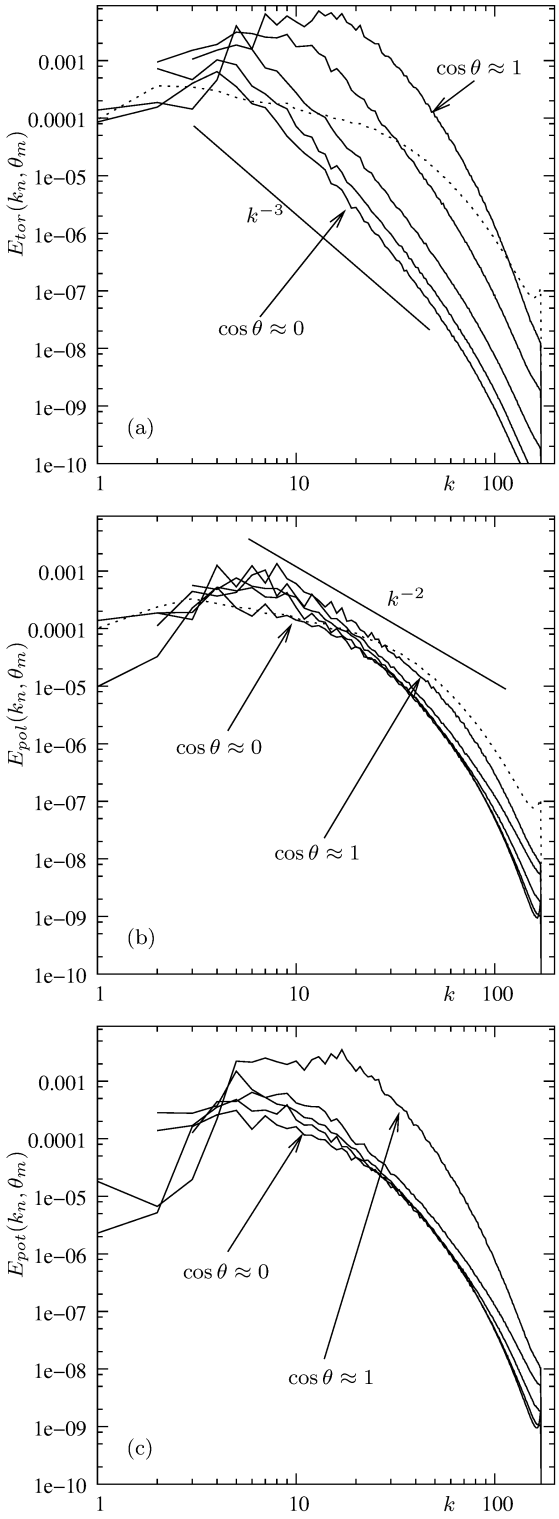

Figure 5: Poloidal (top), toroidal (middle) and potential (bottom) angular spectra for DNS run with $\alpha = 0.1$. Dotted curves show spherical spectra from the corresponding isotropic run for comparison.

The inertio-gravity wave part, consisting of the poloidal and potential modes, shows a collapse and therefore, to some degree, directional isotropy, with a slope close to k^{-2}. Furthermore, apart from the quasi-vertical potential spectrum, poloidal and potential spectra show a high similarity, due to the linear interactions between them. The quasi-vertical potential spectrum dominates over all other wave spectra by more than one order of magnitude at $k \approx 20$, meaning that virtually all the potential energy is found in at $\theta \approx 0$, a significant difference to turbulence with pure stratification. This suggests a linear exchange mechanism in the vertical direction between the potential and toroidal spectrum not existing for pure stratification.

This opens up a mechanism for a faster energy decay, compared to turbulence with pure stratification. Layering of the dominant toroidal part of the energy in vertically de-correlated sheets of horizontal velocities does not allow a direct cascade. The energy in the poloidal and potential parts exhibits a classical cascade with a slope close to k^{-2} for large enough Reynolds numbers. However, the direct link between the potential and the toroidal mode creates a different energy distribution in the poloidal and the potential energies, consecutively allowing a more efficient cascading process of the quasi-vertical toroidal energy. The dependence of these phenomena on non-dimensional parameters such as Froude, Rossby or Reynolds numbers , and the influence of initial equipartition of toroidal, poloidal and potential energy are still to be studied.

CONCLUSIONS

The *linear* evolution of the Eulerian velocity field is completely predictable, as the evolution is determined by its initial conditions. Solutions for the velocity field, but also for higher order velocity correlations are found and so the behaviour of arbitrary Eulerian statistical quantities can in principle be calculated. Within this deterministic picture of the linearized Boussinesq approximation no irreversible anisotropy can be created, only marginal anisotropy through angular phase-mixing of waves, which result from averaging over different $\boldsymbol{k}$-directions. This means that the total—including potential—spectral energy evolution cannot vary and coherent structure formation is inhibited. However, large anisotropic effects can be observed for sets of distinct initial conditions. If these are observed on purpose in DNS or introduced by a not sufficiently careful initialization, needs to be evaluated case by case.

DNS of the Boussinesq equations gives a fully nonlinear evolution of the flow field which naturally develops irreversible anisotropy in the absence of external forcing, i.e. if the energy is allowed to decay freely . The parameter $\alpha = 2\Omega/N$ determines the characteristic evolution of the turbulence. We illustrate two cases:

- $\boldsymbol{\alpha = 0.1}$: dominant stratification with pure rotation initially shows an identical evolution as pure stratification. Pancakes are created in a layered flow, after an initial transient. Due to a factor ten between N and 2Ω we can hardly expect phenomena due to rotation to appear before a time which is tenfold the stratification time scale. This is confirmed by analyzing statistics, such as vorticity correlation length scales, or the Froude number, which exhibit large fluctuations after approximately one system turnover time $2\pi/\Omega$. The effect of rotation after this time is local large production of vorticity, found at small scales. This is confirmed by the evolution of angular spectra, which show a "rising tail", after significantly long simulation times. Visualizations of the iso-enstrophy surfaces at the end of the runs show large flat structures with small scale structures at their sides. The regular pancake pattern has completely disappeared to give place to a strongly intermittent picture. More analysis of these local instabilities is needed. We suspect that one reason for their appearance of these effects is the occurence of unit values of a "local" α, which can be modified by a large coherent vertical vortex. This hypothesis is underlined by the fact that the vertical angular spectrum of the potential energy approaches quantitatively as well as qualitatively the horizontal toroidal spectrum, a tendency also observed for the case $\alpha = 1$.

- $\boldsymbol{\alpha = 10}$: for the toroidal and poloidal part, dominant rotation shows a similar behaviour as pure rotation for short times and a different behaviour at long times. As for the $\alpha = 0.1$ case, the reason for this is the presence of two well-separated time scales of rotation and stratification. However, even at short times, the velocity field is not entirely wave-like, a fraction of the toroidal part is attributed to the vortex mode. Furthermore, energy is also stored in a potential mode, although smaller than the kinetic modes with an approximate ratio of $1/\alpha$. The potential spectra develop a similar anisotropy as the kinetic energy spectra with a dominance in the horizontal direction. This is in contrast to the potential energy spectra of the case $\alpha = 0.1$, where the vertical direction dominates. At large times, the steep spectra due to rotation become less steep for large wave numbers. The effects of this phenomenon on temporal Eulerian statistics are not distinguished. In visualizations, the difference to pure rotation is a significantly increased intermittent behaviour, an observation already made for the $\alpha = 0.1$ case.

Although light is starting to be shed on the physical mechanisms driving rotating and stratified turbulence, a number of questions are still open. Central is the problem of the exact mechanism of decay of anisotropic turbulence, similar to the K41 cascade in isotropic turbulence. Answers can be found by nonlinear modeling or simulations at higher Reynolds numbers, not yet achievable by current computer technology. In the mean time, the parameter space, which is vast in rotating and stratified turbulence, can be further explored. Attention needs to be put on the simulation times, as many physicals phenomena appear only after a number of Brunt-Vaisala frequencies N or rotational frequencies Ω, to be distinguished from numerical artefacts. This is especially true for mixed cases where one of the two is relatively low.

We thank the following computational centers for their generous allocation of resource : IDRIS, operated by CNRS, and CCRT run by CEA.

References

[1] M. Hossain. Reduction in the dimensionality of turbulence due to a strong rotation. *Phys. Fluids*, 6:1077–1080, 1994.
[2] C. Cambon, N. N. Mansour, and F. S. Godeferd. *J. Fluid Mech.*, 337:303–332, 1997.
[3] J.J Riley, R.W. Metcalfe, and M.A. Weissman. DNS of homogeneous turbulence in density-stratified fluids. *Proceedings of AIP Conf. on Nonlinear Properties of Internal Waves*, pages 79–112, New York, 1981.
[4] C. Cambon. *Eur. J. Mech. B - Fluids*, 20:489–510, 2001.
[5] F. S. Godeferd and C. Staquet. *J. Fluid Mech.*, 486:115–150, 2003.
[6] Fabien S. Godeferd and Claude Cambon. *Phys. Fluids*, 6(6):2084–2100, 1994.
[7] F. Bellet, F.S. Godeferd, J.F. Scott, and C. Cambon. Wave-turbulence modelling in rapidly rotating flows. *Advances in Turbulence X, Proc. of ETC10*, 10:337–340, 2004.